First observations of electron gyro-harmonic effects under X-mode HF pumping the high latitude ionospheric F-region

N. F. Blagoveshchenskaya [1], T. D. Borisova [1], A.S. Kalishin [1], T. K. Yeoman [2], I. Häggström [3]

[1] Department of Geophysics, Arctic and Antarctic Research Institute, St. Petersburg, 199397, Russia

[2] University of Leicester, Department of Physics and Astronomy, Leicester LE1 7RH, UK

[3] EISCAT Scientific Association, Kiruna, SE-961 28, Sweden

Correspondence and proofs should be sent to Dr. N. F. Blagoveshchenskaya

Address: Arctic and Antarctic Research Institute, 38, Bering str., St. Petersburg, 199397, Russia

e-mail: nataly@aari.nw.ru

Abstract. We provide the first experimental evidence of the sensitivity of phenomena induced by extraordinary (X-mode) polarized HF high power radio waves to pump frequency stepping across the fifth electron gyro-harmonic (5fce) from below to above. The results were obtained at the EISCAT (European Incoherent Scatter Scientific Association) HF heater facility near Tromsø under effective radiated powers of 456 – 715 MW, when the HF pump wave was transmitted into the magnetic zenith. We have analyzed the behavior and intensities of various spectral lines in the narrowband stimulated electromagnetic emission (SEE) spectra observed far from the heater, HF-enhanced plasma and ion lines (HFPL and HFIL) from EISCAT UHF incoherent scatter radar spectra, and artificial field-aligned irregularities from CUTLASS (Co-operative UK Twin Located Auroral Sounding System) observations, depending on the frequency offset of the pump field relative to the 5fce. At pump frequencies below 5fce the narrowband SEE spectra exhibited very intense so-called stimulated ion Bernstein scatter (SIBS), accompanied by other spectral components, associated with stimulated Brillouin scatter (SBS), which are greatly suppressed and disappeared in the vicinity of 5fce and did not reappear at $f_H > 5$fce. As the pump frequency reached 5fce, the abrupt enhancements of the HFPL and HFIL power, the appearance of cascade lines in the plasma line spectra, and the onset of increasing CUTLASS backscatter power occurred. That is opposite to the ordinary mode (O-mode) effects in the vicinity of 5fce. The X-mode pumping at frequencies below and in the vicinity of the fifth electron gyro-harmonic clearly demonstrated an ascending altitude of generation of induced plasma and ion lines from the initial interaction height, whereas for O-mode heating the region of interaction descended. The observations are consistent with the coexistence of the electron acceleration along and across the geomagnetic field at $f_H < 5$fce, while only very strong electron acceleration along the magnetic field was observed at $f_H \geq 5$fce.

Keywords. Ionosphere (Active experiments), Radio Science (Nonlinear phenomena)

1. Introduction

High-power ordinary mode (O-mode) HF electromagnetic waves radiated from the ground surface are frequently used for the modification of the mid- and high latitude ionosphere F-region. The behaviour and properties of various O-mode HF induced phenomena strongly depend on the proximity of the pump frequency f_H to one of the electron cyclotron harmonics, nfce (fce is the electron gyro frequency and n is the gyro-harmonic number). During last three decades the effects of HF pump frequency stepping through electron gyro-harmonics have been extensively studied at different HF heater facilities located at high and mid latitudes. Gyro-harmonic effects manifest themselves in a great variety of plasma phenomena, induced by non-linear interaction between the ordinary polarized pump wave and ionospheric plasma, such as broadband (classical) stimulated electromagnetic emission (SEE) (*Leyser*, 2001 and references therein ; *Carozzi et al*., 2002; *Kotov et al*., 2008), artificial field-aligned irregularities (FAIs) (*Erukhimov et al*., 1987; *Robinson*, 1989; *Honary et al*., 1999; *Gurevich*, 2007 and references therein; *Frolov et al*., 2012; *Blagoveshchenskaya et al*., 2011; *Borisova et al*., 2014; 2016), HF-induced optical emissions (*Kosch et al*., 2002; 2007; *Mishin et al*., 2005; *Gustavsson et al*., 2006; *Ashrafi et al*., 2007), HF-enhanced ion and plasma lines (HFILs and HFPLs) (*Mishin et al*., 2005; *Borisova et al*., 2014; 2016), narrowband stimulated electromagnetic emission within 1 kHz frequency band (*Bernhardt et al*., 2010; 2011; *Mahmoudian et al*., 2013; *Samimi et al*., 2012; 2013; 2014).

Following standard theory, an X-polarized HF pump wave is not capable of exciting artificial ionospheric turbulence in the F region. The excitation of parametric decay instability requires that the orientation of the electric field of the pump wave at the reflection height should be parallel to the local magnetic field line. This is realized only for O-polarized HF pump waves, while the electric field of the X-mode pump wave is perpendicular to the magnetic field (*Robinson*, 1989; *DuBois et al*., 1990; *Stubbe*, 1996; *Gurevich*, 2007; *Kuo et al.* 2014).

Moreover, the extraordinary polarized powerful radio wave is reflected at a height with the local plasma frequency of $f_{PX}{}^2 = f_H (f_H - fce)$, that is below the electron plasma resonance layer $f_{PO}{}^2 = f_H{}^2$ as well as the upper hybrid resonance layer $f_{PUH}{}^2 = f_H{}^2 - fce^2$, where f_H and fce are the pump frequency and the electron cyclotron frequency respectively. Thus, the X-polarized pump waves should also not generate the thermal parametric (resonance) instability occurring at the UH resonance height (*Grach and Trakhtengerts*, 1975; *Robinson*, 1989; *Gurevich*, 2007). Experiments with the EISCAT (European Incoherent Scatter Scientific Association) HF heater at Tromsø, Norway, concerning the contrasting O/X-mode pumping in the vertical direction at low heater frequencies of 4.544 and 5.423MHz, lying below the maximum plasma frequency of the F2 layer (f_H < foF2), have demonstrated that only O-mode HF pumping is able to induce the generation of the small-scale artificial irregularities in the F2 layer of the ionosphere (*Hedberg et al*., 1983; *Robinson et al*., 1997).

However, a considerable body of repeatable experimental results at EISCAT have clearly indicated that extraordinary polarized high power HF radio waves, injected into the high latitude ionospheric F2 layer towards the magnetic zenith, are capable of generating artificial field-aligned irregularities, radio-induced optical emissions at red (630 nm) and green (557.7 nm) lines, HF-enhanced ion and plasma lines (HFIL and HFPL, which are the signatures of ion acoustic and Langmuir electrostatic waves), and spectral components in the narrowband SEE spectra observed at a large distance from the HF heater (*Blagoveshchenskaya et al.*, 2011; 2013; 2014; 2015). It is important that all the X-mode phenomena listed above at high heater frequencies (f_H = 6 – 8 MHz) are excited under different ratios of the heater frequency to the critical frequency of the F2 layer (f_H /foF2 >1 as well as f_H / foF2≤ 1) (*Blagoveshchenskaya et al.*, 2014; 2015).

We report here for the first time experimental results demonstrating the sensitivity of phenomena induced by extraordinary polarized HF high power radio waves to pump frequency stepping across the fifth electron gyro-harmonic. The results have come from experiments at the

EISCAT HF heater in the course of the pump frequency stepping through the fifth electron gyro harmonic at frequencies below the critical frequency, f_H < foF2 (Section 2). We have analyzed in detail the behavior and intensities of various spectral lines in the narrowband SEE spectra (within 1 kHz around the heater frequency) obtained at a large distance from the Tromsø heater (Section 3.1), HF-enhanced ion and plasma lines from UHF radar spectra (Section 3.2), and artificial field-aligned irregularities from CUTLASS (Co-operative UK Twin Located Auroral Sounding System) observations (Section 3.3), depending on the frequency offset of the pump field relative to the fifth electron gyro-harmonic. The X-mode gyro-harmonic effects near the fifth electron gyro-frequency are compared with those occurred under O-mode HF pumping in the same background conditions (Section 3.4). The results obtained are discussed and summarized in Section 4.

2. General features of experiments

On 25 and 26 October 2013 during a Russian EISCAT campaign, the HF Heater at Tromsø (geographical coordinates 69.6° N, 19.2° E) (*Rietveld et al.*, 1993) was transmitting in a frequency stepping mode in the vicinity of the fifth electron gyro-harmonic frequency (5 fce). Experiments were conducted in the evening hours between 15 and 16 UT in quiet magnetic conditions. The critical frequencies of the F2 layer fall within the range between 7.8 and 8.0 MHz. An X-polarized powerful HF radio wave was pumped into the magnetic zenith (along the geomagnetic field line). The heater duty cycle was 20 min on, 10 min off. In the course of each 20 min heater-on pulse the pump frequency was increased from 6.7 to 6.995 MHz by 5 kHz steps every 20 s. This investigation of the electron gyro-harmonic effects under X-mode HF pumping was performed at heater frequencies below the critical frequency (f_H < foF2).

Previous experiments have demonstrated that an X-mode pumping into the high latitude ionospheric F2 layer along the geomagnetic field line at high heater frequencies (6.2 – 8.0 MHz) leads to the excitation of intense artificial ionospheric turbulences, which were similar in the underdense ionosphere (f_H > foF2) and in the overdense ionosphere (f_H < foF2) (*Blagoveshchenskaya et al*., 2015). In the course of these X-mode electron gyro-harmonic experiments the effective radiated power (ERP) in the geomagnetic field-aligned direction varied between 657 – 715 and 456 – 501 MW in different transmission pulses. The width of the heater beam was about 6° at – 3 dB level. The estimated leakage of the O-mode wave under X-mode HF pumping in the magnetic zenith was about 3.5 - 5 MW.

Table 1 summarizes the general features of X-mode EISCAT/Heating experiments in the vicinity of the fifth electron gyro-harmonic. In addition Table 1 includes the X-mode reflection altitude (h_{refl}) and some parameters obtained from the International Geomagnetic Reference Field (IGRF) model above Tromsø for this altitude, including the geomagnetic field strength B_{0MOD} , ion gyro-frequency for O^+ ions (fci_{MOD}) and the fifth electron gyro-harmonic frequency ($5fce_{MOD}$). The reflection altitude of the X-polarized HF pump wave was derived with the use of the model described by *Borisova et al*. (2002). Electron density profiles Ne(h) above Tromsø, utilized in the model, were taken from EISCAT UHF radar observations just before the transmission pulse, or from ionosonde data. Note, that we were not able to take Ne(h) profiles from UHF radar in the course of heater-on periods due to the strong HF-enhanced ion lines.

Various facilities, including the EISCAT UHF incoherent scatter radar, spatially co-located with the HF heater at Tromsø, the CUTLASS HF coherent radar at Hankasalmi, Finland, and the equipment for the narrowband stimulated electromagnetic emission (SEE) observations near St. Petersburg (at a distance about 1200 km from the HF heater), were utilized as diagnostics for the determination of the distinctive features and behaviors of plasma parameters and artificial ionospheric turbulence, artificial field-aligned irregularities, and narrowband spectral lines depending on the proximity of the pump frequency to the fifth electron gyro-harmonic frequency. Operational details and parameters, derived from the EISCAT UHF and CUTLASS radar measurements, are analogous to those used in *Blagoveshchenskaya et al.*, (2014). A description of the narrowband SEE equipment and its technical features are given in *Blagoveshchenskaya et al.*, (2015).

3. Results of observations

3.1. Narrowband SEE spectral features

On 25 and 26 October 2013 the narrowband stimulated electromagnetic emission (SEE) observations in a 1 kHz frequency band around the heater frequency were conducted near St. Petersburg at a distance of about 1200 km from the Tromsø HF Heating facility, which was operated in the vicinity of the fifth electron gyro-harmonic. In the course of the experiments the frequency stepping was performed at frequencies from 6.7 to 6.995 MHz. During each 20 min transmission pulse the pump frequency was increased by 5 kHz every 20 s. Figure 1 demonstrates the spectrograms of the HF pump wave within ± 250 Hz band taken in the vicinity of St. Petersburg in the course of pump frequency stepping through the fifth electron gyro-harmonic for alternating O- and X-mode heating at Tromsø on 25 and 26 October 2013. The data were obtained with a frequency resolution of 0.2 Hz and time resolution of 5 s. The strong line in the center with zero frequency offset is the pump wave. The SEE band on the spectrograms is represented in such a way that the maximum in the spectrum at the pump frequency corresponded to zero frequency offset at any time. Figure 1 makes it clear that in the course of O-mode pump frequency stepping there were not any spectral structures in the spectrograms. In contrast, all three X-mode pulses (15:31 – 15:51 UT on 25 October 2013 and 15:01 – 15:21 and 15:31 – 15:51 UT on 26 October 2013) exhibit a wide variety of spectral components. Moreover, their behavior with pump frequency stepping from 6.7 to 6.995 MHz in 5 kHz steps was very similar for all X-mode heater-on cycles.

According to the data in Table 1, the reflection altitudes of HF pump wave were between 218 and 223 km in different X-mode pulses. The International Geomagnetic Reference Field

(IGRF) model provides the fifth harmonic of electron gyro-frequencies of 5fce = 6.820 and 6.806 MHz for the altitudes of 218 and 223 km respectively. In the course of the frequency stepping from 6.7 to 6.995 kHz the radiation at 5fce corresponded to 15:09 UT in the transmission pulse on 26 October 2013 from 15:01 – 15:21 UT and 15:38 UT in the transmission pulses from 15:31 – 15:51 UT on 25 as well as on 26 October 2013.

As an example, the behavior of spectral components with pump frequency stepping through the 5fce on 26 October 2013 from 15:01 – 15:21 UT is now considered in more detail. The power spectra, taken for different pump frequency offsets relative to the fifth electron gyro-harmonic frequency (5fce = 6820 kHz) are shown in Figure 2.

As is seen from Figs. 1 and 2, the generation and intensity of spectral lines are strongly affected by the proximity of the pump frequency f_H to the fifth electron gyro-harmonic frequency 5fce. At pump frequencies below the electron gyro-harmonic frequency (f_H < 5fce) the spectra show the discrete downshifted and upshifted harmonic spectral structures separated by about the ion gyro-frequency for O^+ ions (Stokes and anti-Stokes lines). There is an asymmetry in the behavior of electrostatic ion cyclotron (EIC) harmonic waves with respect to the sign of frequency offset. The strength of the main downshifted spectral peak with a frequency offset of – 55.4 Hz was about only 18 - 20 dB below the pump power at heater frequencies below 5fce. In the same conditions the main upshifted spectral line with a peak at + 52.7 Hz had a lower intensity (35 – 40 dB below the pump power). The other spectral line with a frequency offset of – 26.3 Hz and a strength of 20 – 25 dB below the pump power, associated with ion-acoustic (IA) waves, is also seen in the narrowband SEE spectra at f_H < 5fce. This emission coexisted with the ion gyro-harmonic structures.

According to the observations, as the pump frequency approached 5fce, the strength of IA lines start to become suppressed within 15 kHz below 5fce and disappeared at the fifth gyro-harmonic frequency (5fce = 6820 kHz at 15:09 UT on 26 October 2013 in the course of transmission pulse 15:01 – 15:21 UT). At the same time the frequency offset of the downshifted ion-harmonic lines gradually changed from - 55.4 to - 48 Hz and the frequency offset of the upshifted ion -harmonic lines slightly increased from 52.7 to 53.6 Hz. The strength of the upshifted ion gyro-harmonic structures and higher harmonics of the downshifted ion-harmonic lines were suppressed. At 5fce the upshifted EIC harmonic waves disappeared and intensities of the second and third downshifted harmonics were suppressed by 8-10 dB. The disappearance of the ion acoustic line accompanied by the suppressed ion gyro-harmonic structures, recorded far from HF heater facility, can be used as the criteria for determining the electron gyro-harmonic frequency under X-mode HF pumping, when the pump frequency is stepped across the electron gyro-harmonics. In a similar manner, the maximum suppression of the downshifted maximum (DM) component in the classic SEE spectra within few hundred kHz, recorded in the close vicinity of the HF heater, may be utilized for estimating the gyro-harmonic frequency in the course of O-mode experiments (*Leyser*, 2001).

Just above the fifth electron gyro-harmonic (5fce + 10) kHz the transition from discrete lines to a broadband structure occurred. The broadband structure, mainly downshifted relative to the pump frequency, was recorded in the band from – 70 Hz to +50 Hz. It existed above the fifth electron gyro-harmonic in the pump frequency band from 10 to 175 kHz above 5fce. The intensity of the broadband structure maximized under negative frequency offsets. The ion-gyro-harmonic and IA emission lines above 5fce did not reappear in the spectra for f_H = 5fce+ (10 ÷ 175) kHz.

3.2. Artificial ionospheric turbulence

Ordinary polarized (O-mode) high power electromagnetic waves in the vicinity of the reflection altitude decay and couple to high frequency Langmuir waves (L) and low frequency ion-acoustic (IA) waves. This process is called as the parametric decay instability (PDI) (*Perkins et al.*, 1974; *Fejer*, 1979; *Hagfors et al.*, 1983; *DuBois et al.*, 1990; *Stubbe et al.*, 1992; *Kuo et al.*, 2014). Langmuir and ion-acoustic waves in the ionospheric plasma have become a subject of great interest due to the availability of highly detailed experimental results. Incoherent scatter radars provide the direct detection of Langmuir and ion-acoustic waves in the radar spectra as HF-enhanced plasma and ion lines (HFPL and HFIL). The EISCAT UHF radar at 933 MHz was used in the combination with HF heating facility at Tromsø in our X-mode frequency stepping experiments. The turbulence wavelength probed by the EISCAT UHF radar is 0.16 m.

The EISCAT UHF radar was pointing towards the magnetic zenith (186° azimuth, 12° zenith) in all events when the HF pump wave, radiated in the same direction, was stepped across the fifth electron gyro-harmonic. The UHF radar measured the altitudes along the geomagnetic field-aligned direction, $h_{RADAR} = h_{VERT}/\cos 12°$. The pump frequency increased in 5 kHz steps every 20 s that allowed coverage of a bandwidth of 295 kHz during each 20 min transmission pulse. The spectra of Langmuir and ion acoustic plasma waves were derived from “raw” data with 20 s integration time for 3 km altitude steps.

Figure 3 demonstrates the behavior of electron density (Ne) and temperature (Te), raw electron density (backscatter power) and undecoded downshifted plasma line strength from EISCAT UHF radar measurements with 20 s integration time during the HF pumping experiment on 26 October 2013 from 14:30 to 16 UT. The extraordinary (X-mode) polarization was employed in two heater pulses from 15:01 – 15:21 and 15:31 – 15:51 UT. For the comparison, the ordinary (O-mode) polarized pump wave was radiated with the same frequency stepping in the first transmission pulse from 14:31 – 14:51 UT. The X-mode electron gyro-frequency experiment was conducted at pump frequencies below the critical frequency of F2 layer. From Fig. 3 it can be seen that the large Ne enhancements are seen up to altitudes of 650 km through the whole X-mode transmission pulses. These apparent electron density enhancements are a common feature for all X-mode experiments, either those where HF-enhanced ion lines are generated or not (*Blagoveshchenskaya et al*., 2014; 2015). During O-mode cycle from 14:31 – 14:51 UT the apparent Ne increases appeared only in the vicinity of the fifth gyro-resonance frequency and existed at f_H > 5fce to the ending of the pump cycle. The nature of such apparent HF-driven Ne enhancements still remains an unanswered question.

There were no significant changes in the electron temperature behavior as the X-polarized pump wave was stepped in frequency through the 5fce. The strong Te decreases in the vicinity of the gyro-resonances were observed during O-mode injection, which are the typical phenomenon from the UHF radar observations during O-mode gyro-harmonic experiments (*Ashrafi et al*., 2007; *Borisova et al*., 2014; 2016). As is also seen from Fig. 3, the abrupt increases of the backscatter power and undecoded downshifted plasma line strength, which point to the excitation of enhanced ion and plasma lines, were observed when the frequency of X-polarized pump wave achieved the 5fce at 15:09 and 15:38 UT during the transmission pulses from 15:01 – 15:21 and 15:31 – 15:51 UT respectively.

Figure 4 illustrates the altitude distributions of the intensity of the downshifted and upshifted ion lines, and the downshifted plasma line depending on time, obtained with 20 s integration time and the altitude resolution of 3 km, for the same experiment on 26 October 2013. The time-dependence of the critical frequency of the F2 layer foF2 and heater frequencies f_H is also shown. As is evident, in the course of X-mode HF pumping the most intense HFILs and HFPLs were excited from 15:09 – 15:17 and 15:38 – 15:46 UT. It corresponds to the frequency bandwidth of 120 kHz from 5fce to (5fce + 120) kHz. It can be seen that at frequencies above 5fce the downshifted ion lines had two power maxima separated in height by 9 – 12 km. Referring to Figs. 3 and 4, the altitude of generation of HF-induced plasma and ion lines ascended by about 15 km from the initial interaction height during X-mode pumping at frequencies below and in the vicinity of the fifth electron gyro-harmonic, while for O-mode pumping the region of the HFIL and HFPL generation descended by 12 km under the same conditions.

Figure 5 presents more detail of the behavior of plasma and ion line spectra depending on the proximity of the X-mode pump wave frequency to the fifth electron gyro-harmonic frequency taken on 26 October 2013 in the course of the X-mode frequency stepping transmission pulse from 15:01 – 15:21 UT. Spectra are only given at fixed altitudes, in which their power had a maximum. Figure 5 shows the frequency spectra of HF-enhanced downshifted plasma lines and ion lines (HFPL and HFIL), derived for f_H < 5fce (Fig. 5a), f_H = 5fce (Fig. 5b), and f_H > 5fce (Fig. 5c, d, e). At pump frequencies below 5fce (Fig. 5a) by 30 kHz (f_H = 6790 kHz) the downshifted plasma line spectrum (left column) possess a weak peak at zero frequency, corresponding to the heater frequency, and sharp intense peak shifted by the ion-acoustic frequency (f_{IA}) which is proportional to the radar wave number. Typical values for the EISCAT UHF radar are $f_{IA} = \omega_{IA} / 2\pi = 10$ kHz. The ion line spectra (middle column) exhibit two intense shoulders, downshifted and upshifted by the ion-acoustic frequency from zero frequency, and a less pronounced nonshifted peak at zero frequency, corresponding to the radar frequency. The nonshifted feature in the ion spectrum together with the plasma line peak at zero frequency are due to oscillating two stream instability (OTSI). The plasma line peak shifted by the ion-acoustic frequency ("mother" Langmuir wave) together with the ion line shoulders are the signature of the electromagnetic parametric decay instability (PDI).

At the gyro-resonance f_H = 5fce = 6820 kHz (see Fig. 5b) the intensities of plasma and ion lines are greatly increased. The plasma line spectrum clearly demonstrated the so-called downshifted cascade lines at ($\omega_R - (2n + 1)\, \omega_{IA}$) for $n \geq 1$, where ω_R is the radar frequency. Cascade plasma lines show the "daughter" Langmuir waves due to the electrostatic PDI. At pump frequencies above 5fce by 10 and 60 kHz (Fig. 5c, d) plasma and ion line spectra were similar to those observed at 5fce. Again, cascade lines were generated. The first cascade line shows the "mother" Langmuir wave excited by the electromagnetic PDI. The second and third cascade lines are "daughter" Langmuir waves produced by the electrostatic PDI. The strength of plasma and ion lines decreased and the second and third cascade plasma lines were suppressed, when the pump frequency exceeded 5fce by 130 kHz (Fig. 5e).

Plasma and ion line spectra at all altitudes, in which they were excited, derived from UHF radar measurements for different pump frequency offsets relative to the fifth electron gyro-harmonic frequency are shown in Figures 6 and 7 respectively. As is obvious from Figs. 6 and 7, the strength of the HFPLs and HFILs greatly increased at 5fce and was high in the frequency band above 5ce. In the same frequency band the well-defined cascade lines (three lines) were excited in plasma line spectra. The cascade lines can only be excited at different altitudes where their frequency matches the local plasma mode (*Stubbe et al*., 1992). However, the altitude resolution of 3 km, used for the obtaining the plasma line spectra, did not allow the separation of the excitation altitudes of each cascade line. At a pump frequency above 5fce by 60 kHz, two echoes in the downshifted ion line at different heights (see Fig. 7) appeared which existed to the end of transmission cycle. An analogous feature has been observed in other X-mode experiments at pump frequencies of f_H = 7.1 and 6.96 MHz (*Blagoveshchenskaya et al*., 2014; 2015), which are both above fifth electron gyro-harmonic frequency.

3.3. CUTLASS radar backscatter

Artificial field-aligned irregularities (FAIs) are a common feature of EISCAT HF X-mode pumping experiments. As was shown by *Blagoveshchenskaya et al*. (2014; 2015), at high pump frequencies of f_H = 6 – 8 MHz the X-mode FAIs are generated in the high latitude ionospheric F-region both at pump frequencies above and below the critical frequency of the F2 layer. The behavior of X-mode FAIs in the course of HF pump frequency stepping across the fifth electron gyro-harmonic was probed by the CUTLASS (SuperDARN) HF coherent radar at Finland (Lester et al., 2004). Operational details are the same as given in *Blagoveshchenskaya et al*., (2014). Figure 8 depicts the CUTLASS backscatter power in the course of the frequency stepping experiments on 25 and 26 October 2013. CUTLASS operated at frequencies of ~ 16, 18, and 20 MHz implying a transverse size of artificial field-aligned irregularities of $l_\perp \approx$ 9.3, 8.3, and 7.5 m. In Fig.8 the first transmission pulses from 15:01 – 15:21 and 14:31 – 14:51 UT on 25 and 26 October 2013 respectively are shown for O-mode frequency stepping for the comparison between the gyro-harmonic effects observed under the O- and X-mode HF pumping.

Wright et al. (2006) showed that the O-mode FAIs were excited for effective radiated power ERP < 4 MW, which is in the range of the O-mode leakage in our X-mode experiments. CUTLASS observations in the course of O-mode frequency stepping through the electron gyro harmonics clearly demonstrated the suppression of the FAI in the vicinity of the third, fourth and fifth electron gyro harmonic frequency (Honary et al., 1999; Blagoveshchenskaya et al., 2011a, Borisova et al., 2014; 2016). In the course of O-mode heating the power of signals scattered from FAIs is suppressed by 2 – 5 dB as the HF pump frequency reached the 5 fce. The intensity of scattered signals above fifth electron gyro-harmonic frequency (f_H > 5fce) was higher than below 5fce (f_H < 5fce) and reached its maximum at f_H = 5fce + (90 – 120) kHz. As is evident from Fig. 8, the power of signals backscattered from X-mode FAIs increased in the vicinity of the fifth electron gyro-resonance that is opposite to the O-mode effects. The largest enhancements of the backscatter by 10 – 15 dB were observed at higher operational frequencies of ~ 18 and 20 MHz ($l_\perp \approx 8.3$ and 7.5 m). With further increasing the pump frequency, f_H > 5fce + (45 – 60) kHz, the backscatter power gradually decreased and returned to its value before 5fce. Taking into account the different behavior of the CUTLASS backscatter depending on the frequency offset of the pump field relative to the 5fce for O- and X-mode HF pumping, we can conclude that in our experiments gyro-harmonic effects were produced by the X-mode wave but not a small leakage of the O-mode wave. As is also seen from Fig.8, the backscatter power was comparable for O- and X-mode waves. It is unlikely that 3 – 5 MW O-mode wave, corresponding the threshold of the FAI generation, is able to produce the same intensity of scattered signals as was observed for the full O-mode power (ERP = 550 MW).

3.4. Comparison between O- and X-mode gyro-harmonic effects

The narrowband stimulated electromagnetic emission (SEE) spectra, recorded near St. Petersburg at a large distance (about 1200 km) from the Tromsø HF Heater, clearly demonstrated the generation of a wide variety of spectral components in the course of X-mode pumping with the frequency stepping through the fifth electron gyro-harmonic (see Fig.1). The behavior and features of different spectral components are sensitive to the pump frequency relative to 5fce. By contrast, O-mode pulses did not exhibit any spectral structures in the narrowband SEE spectra obtained at a long distance from HF heater.

The behavior and strength of Langmuir and ion acoustic turbulences, excited by an X-polarized pump wave, strongly depended on the proximity of the pump frequency to the fifth electron gyro-harmonic frequency. The strength of the HF-enhanced plasma and ion lines in the UHF radar spectra (HFPL and HFIL) greatly increased at 5fce and stayed high at f_H > 5fce in the frequency band 105 kHz above 5fce. The opposite behavior of HFILs and HFPLs was found in the O-mode frequency stepping experiments near the fifth electron gyro-harmonic. As was shown by *Borisova et al*. [2016], the power of HF-enhanced ion and plasma lines at pump frequencies below the fifth electron gyro-harmonic frequency (f_H < 5fce) was much larger than the power of HFILs and HFPLs at f_H = 5fce and f_H > 5fce. In the course of X-mode pumping at frequencies below and in the vicinity of the fifth electron gyro-harmonic up to f_H = (5fce + 90) kHz the altitude of generation of induced plasma and ion lines ascended by about 15 km from the initial interaction height, while for O-mode pumping the region of interaction descended by about 12 km in the same conditions (see Figs. 3 and 4).

As was shown in the section 3.3., artificial field-aligned irregularities (FAIs) with the spatial scale perpendicular to the magnetic field of $l_\perp \approx (7.5 – 9.3)$ m also exhibited the opposite changes of the CUTLASS backscatter power in the vicinity of the fifth electron gyro-harmonic resonance for X- and O-mode heating (see Fig. 8).

4. Discussion and Summary

We have shown first experimental evidence of the sensitivity of phenomena induced by extraordinary (X-mode) polarized HF high power radio waves to pump frequency stepping across the fifth electron gyro-harmonic (5fce) from below to above. Results come from EISCAT experiments as the frequency of extraordinary HF pump wave was stepped through the fifth electron gyro-harmonic. In the course of the X-mode transmission pulse into the magnetic zenith the pump frequency increased from 6.700 MHz to 6.995 MHz in 5 kHz steps every 20 s. We have considered the electron gyro-harmonic effects from narrowband stimulated electromagnetic emission (SEE) measurements at a distance far from the HF Heater in combination with the EISCAT UHF incoherent scatter radar at 933 MHz, and the CUTLASS Finland (SuperDARN) radar observations.

We have shown that a wide variety of spectral components in the narrowband SEE spectra were recorded, as the pump frequency is stepped through the fifth electron gyro-harmonic. Their behavior and strength are strongly affected by the proximity of the pump frequency f_H to the fifth electron gyro-harmonic frequency, 5fce. At pump frequencies below 5fce (f_H < 5fce) the spectra exhibited four discrete downshifted and upshifted ion-harmonic spectral structures (Stokes and anti-Stokes lines) separated by the ion gyro-frequency, which gradually decayed from the first to the fourth ion harmonic structure. Simultaneously another spectral component, associated with ion-acoustic (IA) waves, was recorded in the SEE spectra.

All observed discrete spectral peaks at f_H < 5fce are completely analogous to those obtained under X-mode pumping at fixed frequency of 7.953 MHz, which was below the sixth electron gyro-harmonic and also recorded near St. Petersburg at a distance of about 1200 km from the Tromsø HF Heating facility (*Blagoveshchenskaya et al*., 2015). There is also a similarity of the discrete spectral lines in the narrowband SEE spectra observed far from the Tromsø HF heater under the X-mode injection to those observed in the close vicinity of the High-frequency Active Auroral Research Program (HAARP) facility in the course of the O-mode heating experiments (*Norin et al*., 2009; *Bernhardt et al*., 2010; 2011; *Samimi et al*., 2012; 2013). Direct parametric decay of the pump electromagnetic wave into ion acoustic and scattered electromagnetic waves via the stimulated Brillouin scatter (SBS) process (*Dysthe et al*., 1977; *Norin et al*., 2009; *Bernhardt, et al*., 2010) can be responsible for the IA emission lines in the narrowband SEE spectra recorded at distance far from the HF heater.

Samimi et al. (2013) suggested a three-step decay process as a generation mechanism of the ion gyro-harmonic structures, so-called stimulated ion Bernstein scatter (SIBS), observed at the HAARP facility under O-mode pumping in the vicinity of the second electron gyro-frequency. First, the powerful electromagnetic (EM) wave is converted to the upper-hybrid or electron Bernstein (UH/EB) electrostatic waves. Then this UH/EB wave decays into another electrostatic UH/EB mode and several neutralized ion Bernstein (IB) waves. In the last step, the newly-generated UH/EB wave, which exhibits a frequency offset equal to the frequency of the neutralized IB modes, is converted back to an EM wave. *Sharma et al*. (1994) proposed the parametric decay instability of extraordinary electromagnetic waves into electrostatic EB and IB waves. Most likely, in our experiments the decay processes occurred at the reflection altitude of the extraordinary HF pump wave. At first, an X-mode wave is reflected from the ionosphere below the upper hybrid resonance altitude. Secondly, the direction of the electric field of the X-mode HF pump wave is perpendicular to the magnetic field in the reflection altitude. Because the electron and ion Bernstein waves are also almost perpendicular to the magnetic field, occurrence of the process at the reflection height seems more reasonable than the upper hybrid altitude. The production of SIBS structures is an indication of strong electron acceleration across the magnetic field by the EB waves (*Samimi et al*., 2014).

At pump frequencies below the fifth electron gyro-harmonic frequency (f_H < 5fce) the generation of the SIBS structures in the narrowband SEE spectra was accompanied by excitation of enhanced plasma and ion lines from the EISCAT UHF radar measurements, which are signatures of Langmuir and ion-acoustic waves, as well as field-aligned artificial irregularities ($l_\perp$

≈ 7.5 – 9.3 m) from the CUTLASS (SuperDARN) observations. Langmuir waves could cause the electron acceleration along the magnetic field and electron density enhancements (*Carlson et al.*, 1982; *Gurevich et al*., 2004; *Gurevich*, 2007). The typical feature in the behavior of Langmuir and ion-acoustic waves was the gradual ascending of their generation altitude by 15 km from the initial interaction height, when an X-mode HF pumping was carried out below and in the vicinity of the fifth electron gyro-harmonic, while for O-mode pumping the region of the HFIL and HFPL generation descend by 12 km in the same conditions. As was shown by *Kuo et al.* (2010), X-mode heating at HAARP moves the ionosphere upward, whereas O-mode pumping moves the ionosphere downward. In the course of the EISCAT X-mode HF pumping the electron density profiles from the EISCAT UHF radar measurements have also demonstrated the altitude ascending of the Ne peak in the F-region of the ionosphere (*Blagoveshchenskaya et al*., 2013).

Drastic changes in the behavior of the narrowband spectral structures, Langmuir and ion-acoustic turbulences, and FAIs occurred as the frequency of the X-polarized pump wave reached the fifth electron gyro-harmonic. SBS emission lines in the narrowband SEE spectra disappeared and SIBS structures are first greatly suppressed and then they also disappeared just above the fifth electron gyro-harmonic frequency, (5fce + 10) kHz. Moreover, at pump frequencies above the fifth electron gyro-harmonic, discrete structures in the narrowband SEE spectra (SBS and SIBS) did not reappear. Taking into account that the production of SIBS structures points to strong electron acceleration across the magnetic field (*Samimi et al*., 2014), we conclude that the electron acceleration across the magnetic field line is strongly reduced at f_H = 5fce and f_H > 5fce.

The abrupt increases of Langmuir and ion-acoustic wave intensities, that is evident from UHF radar spectra as enhanced plasma and ion lines (HFPL and HFIL), occurred as the pump frequency reached the fifth electron gyro-harmonic frequency. In addition, the plasma line spectrum clearly exhibited the downshifted cascade lines (three lines). The first cascade line was generated due to electromagnetic PDI, when the high-power electromagnetic wave decayed into electrostatic “mother” Langmuir wave and ion-acoustic wave, EM → L + IA. If the “mother”

Langmuir waves carry enough energy, they can encounter further decay cascades according to L → L' + IA' and L' → L" + IA" produced by the electrostatic PDI, until these processes become prohibited by kinematic effects. Analytical estimates and numerical simulations (*Krafft and Volokitin*, 2016) have shown that the “daughter” Langmuir waves L' and L" can accelerate the flux of electrons. In addition, this process can be particularly efficient if scattering effects of waves on plasma irregularities have already accelerated a sufficient flux of electrons (*Krafft and Volokitin*, 2016). The plasma line spectra stayed similar to those observed at 5fce in the frequency band of ~100 - 120 kHz above 5fce. Therefore, the excitation of intense Langmuir waves (L, L', L") points to the enhancement of the electron acceleration along the magnetic field line at f_H = 5fce and f_H > 5fce as compared with the case of f_H < 5fce.

In the same pump frequency band between f_H = 5fce and f_H = 5fce + (100 – 120) kHz the ion line spectra exhibit a strong asymmetry between the downshifted and upshifted shoulders and a large altitude spreading of the HF-enhanced IA layer. Moreover, two maxima in the altitude distribution of the downshifted ion line powers appeared at pump frequencies above the fifth electron gyro-harmonic frequency by 60 kHz, which existed up to the ending the pump frequency stepping cycle, when f_H = 5fce + 175 kHz. The bottom IA layer was observed near the reflection altitude of the extraordinary polarized powerful HF radio wave, whereas the top IA layer was 12 km above the bottom one. All these features mentioned above can be produced by burned out collapsing cavities and the heat flux-driven instability (*Mishin et al*., 2016).

As was shown by *Borisova et al*. (2016), the opposite behavior of HFILs and HFPLs was found in the O-mode frequency stepping through the fifth electron gyro-harmonic. In the course of the O-mode frequency stepping the intensity of HFPLs and HFILs at f_H < 5fce was much stronger than at the fifth electron gyro-harmonic frequency and above it, as opposed to the X-mode experiments in the vicinity of 5fce. Moreover, the X-mode pumping at frequencies below and in the vicinity of the fifth electron gyro-harmonic demonstrated that the generation altitude of induced plasma and ion lines ascended by about 15 km from the initial interaction height, whereas for O-mode pumping the region of interaction descended by about 12 km in the same conditions.

It is common knowledge that an extraordinary polarized HF pump wave cannot parametrically excite the longitudinal electrostatic plasma waves, such as Langmuir and ion-acoustic waves, due to it not possessing an electric field component parallel to the geomagnetic field direction near the reflection altitude, and the fact that it does not satisfy the frequency matching condition. Recent investigations of *Wang et al*. (2016) have theoretically demonstrated, that during propagation the X-mode HF pump wave may develop a small parallel electric field component of sufficient magnitude to exceed the parametric decay instability threshold, because the ionosphere is an inhomogeneous and dispersive medium. In such a case, the dispersive effect of the inhomogeneous plasma redirects a small portion of the pump wave field in a direction parallel to the geomagnetic field. It could be a reasonable explanation of the parametric decay instability excitation by X-mode HF pump wave at heater frequencies below the critical frequency of the F2 layer (f_H < foF2). However, why the small portion of the pump wave in a direction parallel to the magnetic field line and full power O-mode heating manifest the opposite behavior of HFPLs and HFILs relative to the proximity of the pump wave frequency to 5fce is unknown.

Behavior of artificial field-aligned irregularities (FAIs) with the spatial scale across the geomagnetic field of $l_\perp \approx (7.5 – 9.3)$ m, excited by X-mode HF pumping into the high latitude ionospheric F-region, is sensitive to the pump frequency relative to the fifth harmonic of the electron gyro-frequency. The CUTLASS backscatter power began to increase at the fifth electron gyro-harmonic frequency and peaked at f_H = (5fce + (45 - 60)) kHz. An increase of 10 – 15 dB was seen at higher operational frequencies of ~ 18 and 20 MHz ($l_\perp \approx 8.3$ and 7.5 m). By a contrast to the O-mode field-aligned irregularities, the X-mode FAIs are not associated with upper hybrid waves. The extraordinary polarized powerful radio wave is reflected below the upper hybrid resonance. Thus, the X-polarized pump waves should not generate the thermal parametric (resonance) instability occurring at the UH resonance height (*Grach and Trakhtengerts*, 1975; *Robinson*, 1989; *Gurevich*, 2007). Moreover, the X-mode FAIs can be excited at the heater frequencies above the critical frequency of the F2 layer, when O-mode heating effects are impossible (*Blagoveshchenskaya et al.*, 2015). In this respect one would expect that the generation mechanism of the X-mode FAIs is related to and driven by the HF-induced large-scale artificial irregularities, which are generated by the growth of a self-focusing instability of HF beam at the heater frequencies above and below the critical frequency (*Kuo et al*., 2010; *Gurevich*, 2007). However, the generation mechanism of the X-mode FAIs is still remains an open question. Similar to the behavior of enhanced plasma and ion line, the opposite changes of the backscatter power relative to the proximity of the pump frequency to 5fce, were observed under O-mode heating. The O-mode FAIs were suppressed by 2 – 5 dB during heating near the fifth harmonic of electron gyro-frequency. The suppression of FAIs at frequencies close to the third or higher electron gyro-harmonics is a typical feature of the O-mode heating. This suppression results in the reduced ability of FAIs to trap the upper hybrid electrostatic waves near the electron gyro-frequencies (*Mjølhus*, 1993).

Acknowledgements. EISCAT is an international scientific association supported by research organizations in China (CRIRP), Finland (SA), Japan (NIPR and STEL), Norway (NFR), Sweden (VR), and the United Kingdom (NERC). CUTLASS is supported by the UK Science and Technology Facilities Council Grant PP/E007929/1, the Finnish Meteorological Institute, and the Swedish Institute of Space Physics. TKY is supported by UK NERC grant NE/K011766/1. We thank Dr. M. Rietveld for help with EISCAT HF pumping experiments and calculations of the effective radiated power.

References

Ashrafi, M., Kosch, M. J., Kaila, K., Isham. B., 2007. Spatiotemporal evolution of radio wave pump-induced ionospheric phenomena near the fourth electron gyroharmonic. J. Geophys. Res. 112, A05314, doi:10.1029/2006JA011938.

Bernhardt, P. A., Selcher, C.A., Lehmberg, R.H., Rodriguez, S.P., Thomason, J.F., Groves, K.M., McCarrick, M.J., Frazer, G.J., 2010., Stimulated Brillouin Scatter in a magnetized ionospheric plasma. Phys. Rev. Lett. 104, 165004, doi:10.1103/PhysRevLett.104.165004.

Bernhardt, P.A., Selcher, C. A., Kowtha, S., 2011. Electron and ion Bernstein waves excited in the ionosphere by high power EM waves at the second harmonic of the electron cyclotron frequency. Geophys. Res. Lett. 38, doi:10.1029/2011GL049390.

Blagoveshchenskaya, N. F., Borisova, T.D, Yeoman, T. K., Rietveld, M. T., 2011a. The effests of modification of a high-latitude ionosphere by high-power HF radio waves. Part 1. Results of multi-instrument ground-based observations. Radiophys. Quant. Electron. (Engl. Transl.). 53, (9-10), 512 – 531.

Blagoveshchenskaya, N. F., Borisova, T. D., Yeoman, T., Rietveld, M. T., Ivanova, I.M., Baddeley, L.J., 2011b. Artificial field-aligned irregularities in the high-latitude F region of the ionosphere induced by an X-mode HF heater wave. Geophys. Res. Lett. 38, L08802, doi: 10.1029/2011GL046724.

Blagoveshchenskaya, N. F., Borisova, T. D., Yeoman, T. K., Rietveld, M. T., Häggström, I., Ivanova, I. M., 2013. Plasma modifications induced by an X-mode HF heater wave in the high latitude F region of the ionosphere. J. Atmos. Sol.-Terr. Phys. 105-106, 231 - 244.

Blagoveshchenskaya, N. F., Borisova, T. D., Kosch, M., Sergienko, T., Brändström, U., Yeoman, T.K., Häggström, I., 2014. Optical and Ionospheric Phenomena at EISCAT under Continuous X-mode HF Pumping. J. Geophys. Res.: Sp. Phys. 119, 10,483–10,498, doi:10.1002/ 2014JA020658.

Blagoveshchenskaya, N.F., Borisova, T.D., Yeoman, T.K., Häggström, I., Kalishin, A.S., 2015. Modification of the high latitude ionosphere F region by X-mode powerful HF radio waves: Experimental results from multi-instrument diagnostics. J. Atmos. Sol.-Terr. Phys. 135, 50–63.

Borisova, T. D., Blagoveshchenskaya, N. F., Moskvin, I. V., Rietveld, M. T., Kosch, M. J., Thidé, B., 2002. Doppler shift simulation of scattered HF signals during the Tromsø HF pumping experiment on 16 February 1996. Ann. Geophys. 20, 1479–1486.

Borisova, T. D., Blagoveshchenskaya, N. F., Kalishin, A.S., Kosch, M., Senior, A., Rietveld, M.T., Yeoman, T.K., Hägström, I., 2014. Phenomena in the high-latitude ionospheric F region induced by a HF heater wave at frequencies near the fourth electron gyroharmonic. Radiophys. Quant. Electron. (Engl. Transl.). 57(1), 1-19.

Borisova, T. D., Blagoveshchenskaya, N. F., Kalishin, A.S., Rietveld, M.T., Yeoman, T.K., Hägström, I., 2016. Modification of the high-latitude ionospheric F region by high-power HF radio waves at frequencies near the fifth and sixth electron gyroharmonics. Radiophys. Quant. Electron. (Engl. Transl.). 58(8), 561 - 585.

Carlson, H. C., Wickwar, V. B., Mantas, G. P., 1982. Observations of fluxes of suprathermal electrons accelerated by HF excited instabilities. J. Atmos. Terr. Phys. 44, 1089–1100.

Carozzi, T. D., Thidé, B., Grach, S. M., Leyser, T. B., Holtz, M., Komrakov, G. P., Frolov, V. L., Sergeev, E. N., 2002. SEE during frequency sweep through fourth electron gyroharmonic. J. Geophys. Res. 107(A9), 1253, doi:10.1029/2001JA005082.

DuBois, D. F., Rose, H. A., Russell, D., 1990. Excitation of strong Langmuir turbulence in plasmas near critical density: Application to HF heating of the ionosphere. J. Geophys. Res. 95, 21221 – 21272.

Dysthe, K.B., Leer, E., Trulsen, J., Stenflow, L., 1977. Stimulated Brillouin Scattering in the ionosphere. J. Geophys Res. 82, 717-718.

Erukhimov, L.M., Metelev, S.A., Myasnikov, E.N., Mityakov, N.A., Frolov, V.L., 1987. Artificial ionospheric turbulence (review). Radiophys. Quant. Electron. (Engl. Transl.). 31, 156 – 171.

Fejer, J.A.,1979. Ionospheric Modification and Parametric Instabilities. Rev. Geophys. Space Phys., 17 (1), 135 - 153.

Frolov, V. L., Bolotin, I. A., Komrakov, G.P., et al., 2012. Gyroharmonic features of the HF-induced ionospheric irregularities. Radiophys. Quant. Electron. (Engl. Transl.). 55(6), 357 - 381.

Grach, S. M., Trakhtengerts, V. Y., 1975. Parametric excitation of ionospheric irregularities extended along the magnetic field. Radiophys. Quant. Electron. (Engl. Transl.). 18, 951–957.

Gustavsson, B., Leyser, T. B., Kosch, M., Rietveld, M. T., Steen, Å, Brändström, B. U. E., Aso, T., 2006. Electron gyroharmonic effects in ionization and electron acceleration during high-frequency pumping in the ionosphere. Phys. Rev. Lett., 97, 195002, doi:10.1103/PhysRevLett.97.195002.

Gurevich, A.V., Carlson, H.C., Medvedev, Yu.V., Zybin, K.R., 2004. Langmuir turbulence in ionospheric plasma. Phys. Rep. 30, 995-1005.

Gurevich, A. V., 2007. Nonlinear effects in the ionosphere. Physics-Uspekhi. 50, 1091–1121.

Hagfors, T., Kofman, W., Kopka, H., Stubbe, P., Ijnen, T., 1983. Observations of enhanced plasma lines by EISCAT during heating experiments. Radio Sci. 18, 861 – 866.

Hedberg, Å., Derblom, H., Thidé, B., Kopka, H., Stubbe, P., 1983. Observations of HF backscatter associated with the heating experiment at Tromsø. Radio Sci., 18 (6), 840 – 850.

Honary, F., Robinson, T.R., Wright, D.M., Stocker, A.J., Rietveld, M.T., McCrea, I., 1999. First direct observation of the reduced striations at pump frequencies close to the electron gyroharmonics. Ann. Geophys. 17, 1235–1238.

Kosch, M. J., Rietveld, M. T., Kavanagh, A. J., Davis, C., Yeoman, T. K., Honary, F., Hagfors, T., 2002. High-latitude pump-induced optical emissions for frequencies close to the third electron gyro-harmonic. Geophys. Res. Lett. 29(23), 2112, doi:10.1029/2002GL015744.

Kosch, M. J., Pedersen, T., Mishin, E., Oyama, S.-I., Hughes, J., Senior, A., Watkins, B., Bristow, B., 2007. Coordinated optical and radar observations of ionospheric pumping for a frequency pass through the second electron gyro-harmonic at HAARP. J. Geophys. Res. 112, A06325, doi:10.1029/2006JA012146.

Kotov, P. V., Sergeev, E. N., Grach, S. M., 2008. Spectra of stimulated electromagnetic emission of the ionosphere upon sweeping of the pump wave frequency near gyroharmonics. I. Experimental results. Radiophys. Quant. Electron. (Engl. Transl.). 51, 417–430.

Krafft, C., Volokitin, A. S., 2016. Electron acceleration by Langmuir waves produced by a decay cascade. Astrophys. Journal, 821:99 (10pp), doi:10.3847/0004-637X/821/2/99.

Kuo, S., Cheng, W.-T., Snyder, A., Kossey, P., Battis, J., 2010. Contrasting O/X-mode heater effects on O-mode sounding echo and the generation of magnetic pulsations. Geophys. Res. Lett. 37, L01101, doi: 10.1029/2009GL041471.

Kuo, S., Snyder, A., Lee, M. C., 2014. Experiments and theory on parametric instabilities excited in HF heating experiments at HAARP. Phys. Plasmas. 21, 062902, doi: 10.1063/1.4885642.

Lester, M., et al., 2004. Stereo CUTLASS: A new capability for the SuperDARN radars. Ann. Geophys., 22, 459 -473.

Leyser, T. B., 2001. Stimulated electromagnetic emissions by high-frequency electromagnetic pumping of the ionospheric plasma. Space Sci. Rev. 98, 223 – 328.

Mahmoudian, A., Scales, W.A., Bernhardt, P.A., Fu, H., Briczinski, S.J., McCarrick, M.J., 2013. Investigation of ionospheric stimulated Brillouin scatter generated at pump frequencies near electron gyroharmonics. Radio Sci. 48, 685697, doi:10.1002/2013RS005189.

Mishin, E. V., Kosch, M. J., Pedersen, T. R., Burke, W. J., 2005. HF-induced airglow at magnetic zenith: Thermal and parametric instabilities near electron gyroharmonics. Geophys. Res. Lett. 32, L23106, doi:10.1029/2005GL023864.

Mishin, E., Watkins, B., Lehtinen, N., Eliasson, B., Pedersen, T., Grach, S., 2016. Artificial ionospheric layers driven by high-frequency radiowaves: An assessment. J. Geophys. Res.: Sp. Phys. 121, doi:10.1002/2015JA021823.

Mjølhus, E., 1993. On the small scale striation effect in ionospheric radio modification experiments near harmonics of the electron gyrofrequency. Radio Sci. 25, 1321– 1339.

Norin, L., Leyser, T.B., Nordblad, E., Thidé, B., McCarrick, M., 2009. Unprecedentedly strong and narrow electromagnetic emissions stimulated by high-frequency radio waves in the ionosphere. Phys. Rev. Lett. 102, 065003, doi:PhysRevLett102.065003.

Perkins, F.W., Oberman, C., Valco, E.J., 1974. Parametric instabilities and ionospheric modification. J. Geophys. Res. 79, 1478 – 1496.

Rietveld, M. T., Kohl, H., Kopka, H., Stubbe, P., 1993. Introduction to ionospheric heating at Tromsø – I. Experimental overview. J. Atmos. Sol. Terr. Phys. 55. 577 - 599.

Robinson, T.R., 1989. The heating of the high latitude ionosphere by high power radio waves. Phys. Rep. 179, 79 – 209.

Robinson, T.R., Stocker, A.J., Bond, G.E., Eglitis, P., Wright, D.M., Jones, T.D., 1997. O-and X-mode heating effects observed simultaneously with the CUTLASS and EISCAT radars and low power HF diagnostic at Tromsø. Ann. Geophys. 15, 134 - 136.

Samimi, A., Scales, W. A., Bernhardt, P. A., Briczinski, S. J., Selcher, C. A., McCarrick, M. J., 2012. On ion gyro-harmonic structuring in the stimulated electromagnetic emission spectrum during second electron gyro-harmonic heating. Ann. Geophys., 30, 1587–1594.

Samimi, A., Scales, W.A., Fu, H., Bernhardt, P.A., Briczinski, S.J., McCarrick, M. J., 2013. Ion gyroharmonic structures in stimulated radiation during second electron gyroharmonic heating: 1. Theory. J. Geophys. Res.: Sp. Phys. 118, 502-514, doi:10.1029/2012JA018146.

Samimi, A., Scales, W.A., Bernhardt, P.A., Briczinski, S.J., McCarrick, M.J., 2014. Ion gyroharmonic structures in stimulated radiation during second electron gyroharmonic heating: 2. Simulations. J. Geophys. Res.: Sp. Phys. 119, doi:10.1002/2013JA019341.

Sharma, R. P., Kumar, A., Kumar, R., Tripathi, Y.K., 1994. Excitation of electron Bernstein and ion Bernstein waves by extraordinary electromagnetic pump: Kinetic theory. Phys. Plasmas. 1(3), 522 – 527, DOI:10.1063/1.870796.

Stubbe, P., Kohl, H., Rietveld, M.T., 1992. Langmuir turbulence and ionospheric modification. J. Geophys. Res. 97, 6285 – 6297.

Stubbe P., 1996. Review of ionospheric modification experiments at Tromsø. J. Atmos. Terr. Phys., 58, 349 – 368.

Wang, X., Cannon, P., Zhou, C., Honary, F., Ni, B., Zhao, Z., 2016. A theoretical investigation on the parametric instability excited by X-mode polarized electromagnetic wave at Tromsø. J. Geophys. Res.: Sp. Phys. 121, doi:10.1002/2016JA022411.

Wright, D. M., Davies, J. A., Yeoman, T. K., Robinson, T. R., and Shergill, H., 2006. Saturation and hysteresis effects in ionospheric modification experiments observed by the CUTLASS and EISCAT radars. Ann. Geophys., 24, 543–553.

Table 1. General features of EISCAT/Heating experiments carried out in the course of the X-mode HF pumping at frequency stepping through the fifth electron gyro-harmonic.

Date, time (UT) of heater pulse	ERP, MW	Range of f_H stepping, MHz	foF2, MHz	hrefl, km	B_{0MOD}, nT	$fci(O+)_{MOD}$, Hz	$5fce_{MOD}$, MHz
26 Oct 2013 15:01 – 15:21	650 - 715	6.700 – 6.995	7.9	218	48733.2	46.8	6,820
26 Oct 2013 15:31 – 15:51	450 - 500	6.700 – 6.995	7.9	223	48633.6	46.7	6.806
25 Oct 2013 15:31 – 15:51	450 - 500	6.700 – 6.995	7.8	223	48633.5	46.7	6.806

Figure captions

Figure 1. The spectrogram of the narrowband SEE structures recorded with a frequency resolution of 0.2 Hz and time resolution of 5 s at a distance of 1200 km from the EISCAT/Heating for contrasting O/X-mode HF pumping on 25 and 26 October 2013 in the course of the pump frequency stepping across the fifth electron gyro-harmonic. The strong line in the center with zero frequency offset is the pump wave. The SEE band is represented in such a way that the maximum in the spectrum at the pump frequency corresponded to zero frequency offset at any time. Arrows indicate the time, when f_H = 5fce.

Figure 2. Narrowband SEE spectra, showing the downshifted and upshifted ion gyro-harmonic and downshifted ion-acoustic structures taken for different pump frequency offsets relative to the fifth electron gyro-harmonic frequency during the X-mode frequency stepping pulse from 15:01 – 15:21 UT on 26 October 2013. The value of 5fce was 6820 kHz.

Figure 3. The behavior of the electron density (Ne) and temperature (Te), the raw electron density (backscattered power) and undecoded downshifted plasma line strength from EISCAT UHF radar measurements with 20 s integration time during HF frequency stepping across 5fce from below to above on 26 October 2013. The O-mode wave was radiated from 14:31 – 14:51 UT, and X-mode polarization was employed from 15:01 – 15:21 and 15:31 – 15:51 UT. The arrows on the time axis indicate the time when f_H = 5fce.

Figure 4. The altitude distributions of the intensity of the downshifted and upshifted ion lines, and the downshifted plasma line, depending on time, obtained with 20 s integration time and an altitude resolution of 3 km, for the same experiment as in Fig.3 The behavior in time of the

critical frequency of the F2 layer foF2 and heater frequencies f_H is also shown in the bottom panel.

Figure 5. Plasma (left column) and ion line (middle and right columns) spectra derived from the raw EISCAT UHF radar measurements with 20 s integration time and 3 km height resolution depending on the proximity of the X-mode pump wave frequency to the fifth electron gyro-harmonic frequency, taken on 26 October 2013 in the course of the X-mode frequency stepping transmission pulse from 15:01 – 15:21 UT. Spectra are given at fixed altitudes, in which their power had a maximum. Spectra were derived for the different pump frequency offsets relative to 5fce: f_H < 5fce (a), f_H = 5fce (b), and f_H > 5fce(c, d, e).

Figure 6. Plasma line spectra at all altitudes, in which they were excited, derived from the raw EISCAT UHF radar measurements with 20 s integration time and 3 km height resolution for different pump frequency offsets relative to the fifth electron gyro-harmonic frequency during the X-mode frequency stepping pulse from 15:01 – 15:21 UT on 26 October 2013. The value of 5fce was 6820 kHz.

Figure 7. Ion line spectra at all altitudes, in which they were excited, derived from the raw EISCAT UHF radar measurements for the same heater pulse and pump frequency offsets relative to the fifth electron gyro-harmonic frequency as the plasma line spectra in Fig. 6.

Figure 8. CUTLASS radar backscatter (Hankasalmi, Finland, the beam 5 oriented at the artificially disturbed ionosphere region over Tromsø) at three operational frequencies (~ 16, 18, and 20 MHz) for contrasting O/X-mode pump frequency stepping across the fifth electron gyro-harmonic on 25 October 2013 (a) and 26 October 2013 (b). The dynamics of the backscatter powers averaged between 29 – 35 gates is depicted in the top panels and their dynamics

depending on the range gate and UT time is illustrated in the bottom panels. Heater cycles and polarization of the pump wave are marked on the time axis. Arrows indicate the time when f_H = 5fce.

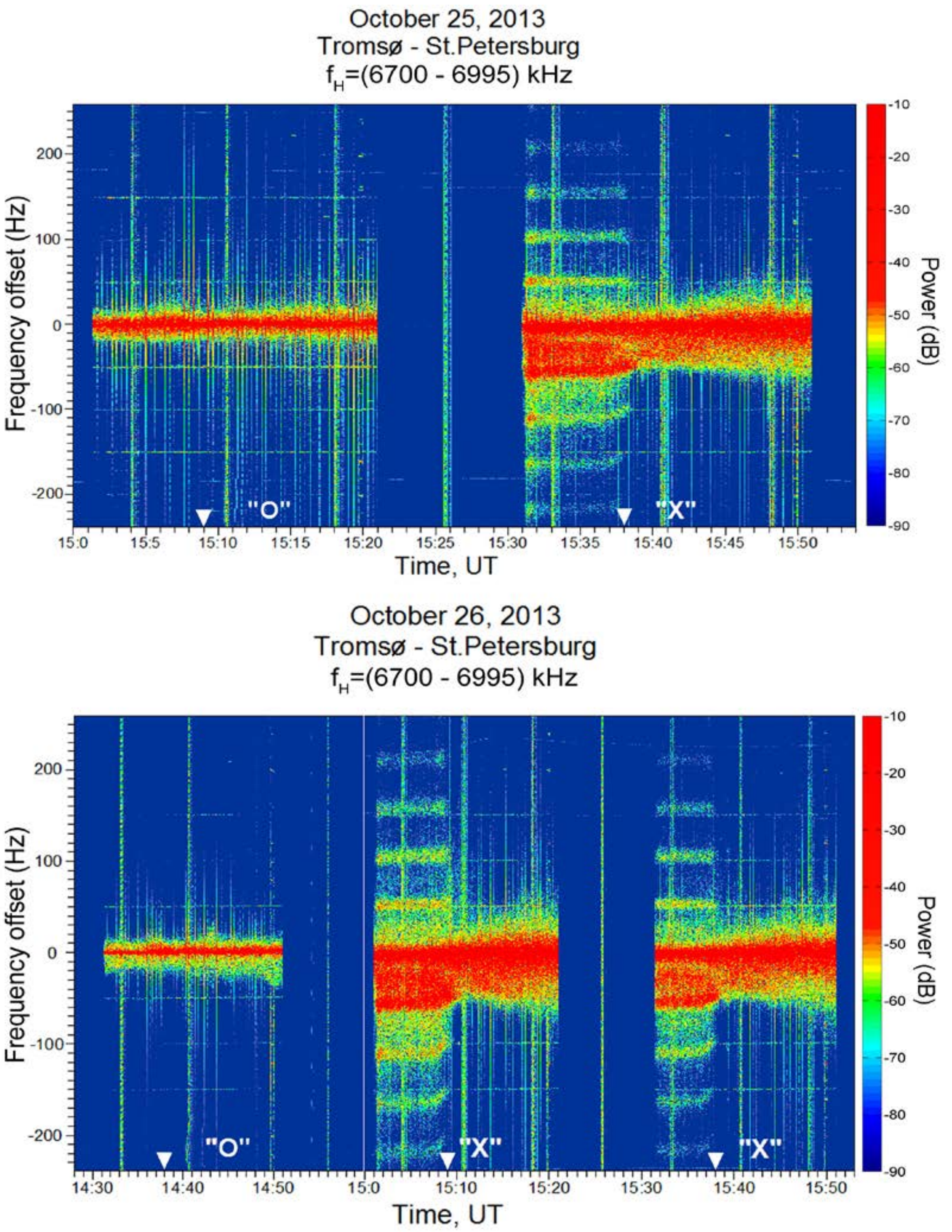
October 25, 2013
Tromsø - St.Petersburg
f_H=(6700 - 6995) kHz
Frequency offset (Hz)
Time, UT
Power (dB)
"O"
"X"
October 26, 2013
Tromsø - St.Petersburg
f_H=(6700 - 6995) kHz
Frequency offset (Hz)
Time, UT
Power (dB)
"O"
"X"
"X"

Figure 1.

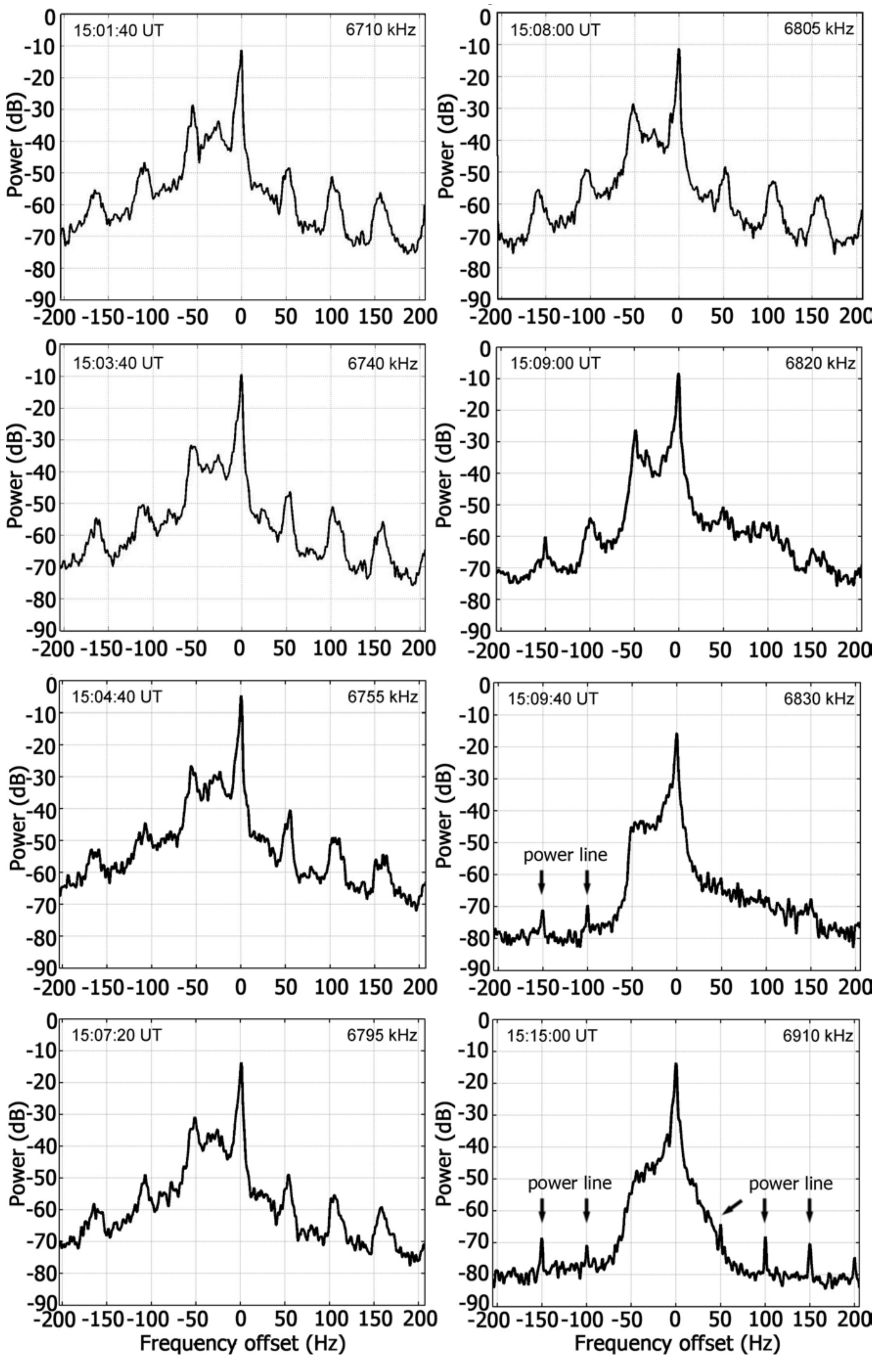

15:01:40 UT
6710 kHz
15:08:00 UT
6805 kHz
15:03:40 UT
6740 kHz
15:09:00 UT
6820 kHz
15:04:40 UT
6755 kHz
15:09:40 UT
6830 kHz
power line
15:07:20 UT
6795 kHz
15:15:00 UT
6910 kHz
power line
power line
Power (dB)
Frequency offset (Hz)

Figure 2.

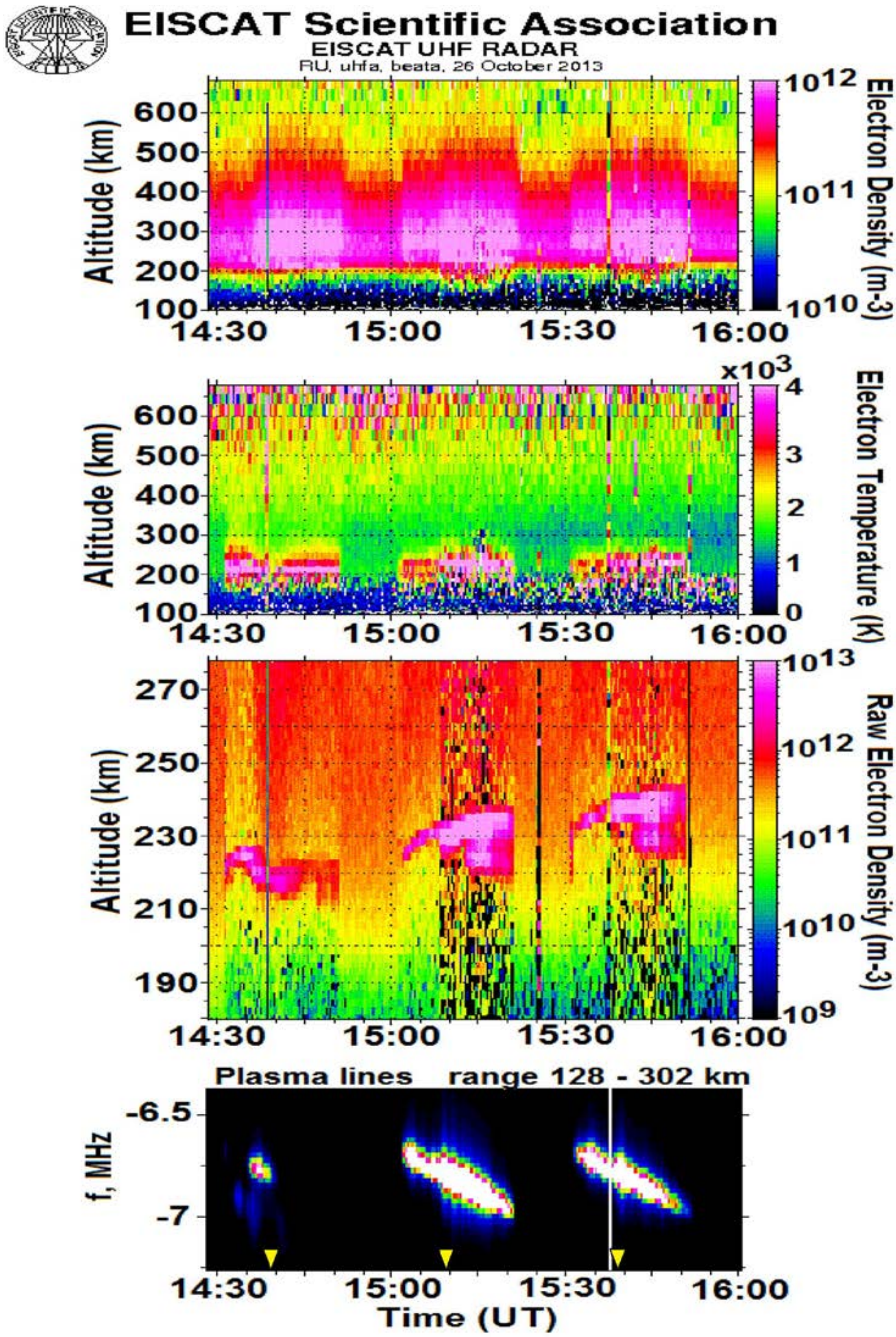
EISCAT Scientific Association
EISCAT UHF RADAR
RU, uhfa, beata, 26 October 2013
Altitude (km)
Electron Density (m-3)
Electron Temperature (K)
Raw Electron Density (m-3)
Plasma lines range 128 - 302 km
f, MHz
Time (UT)

Figure 3.

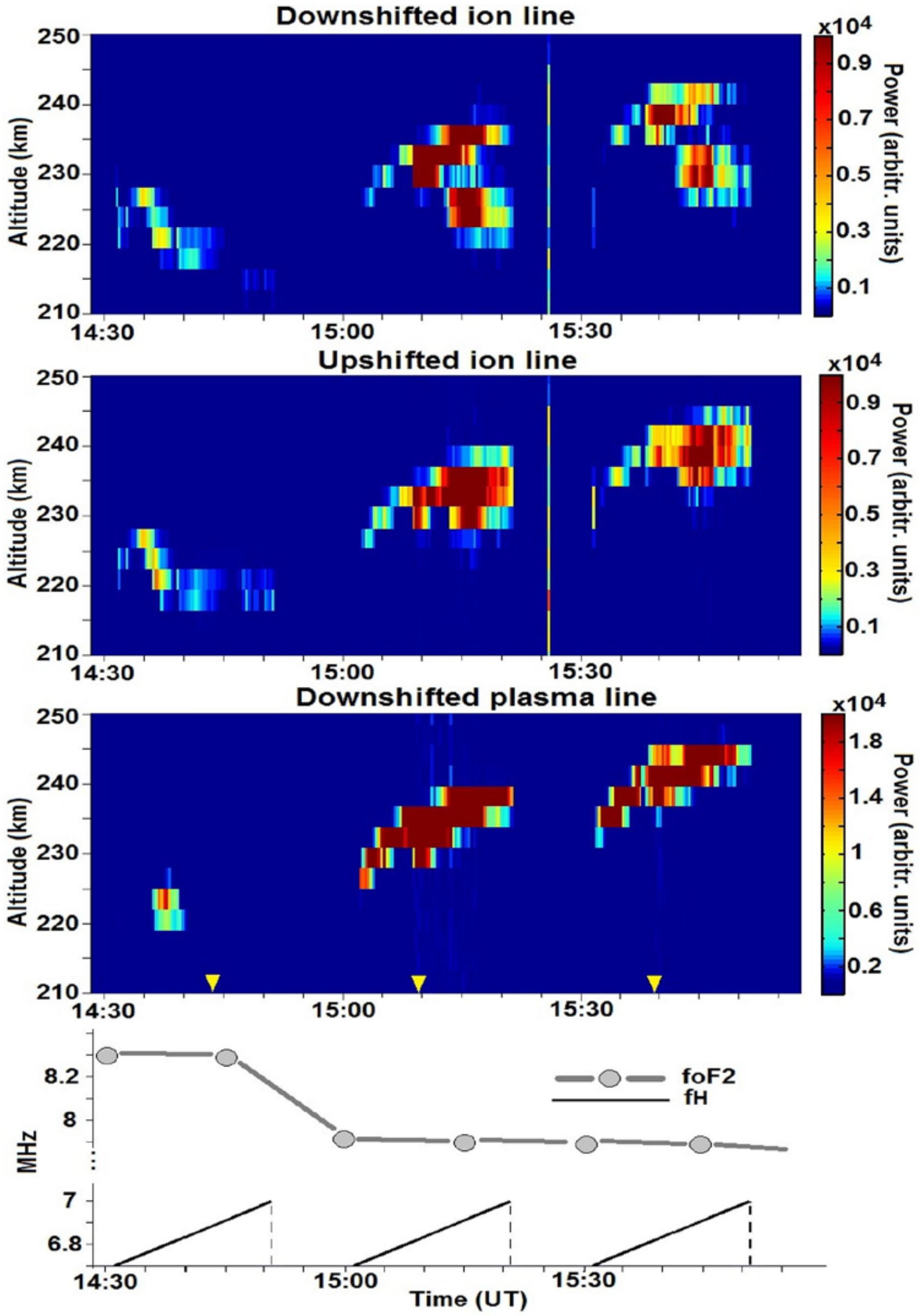

Downshifted ion line
Upshifted ion line
Downshifted plasma line
Altitude (km)
Power (arbitr. units)
x10^4
foF2
fH
MHz
Time (UT)
14:30
15:00
15:30

Figure 4.

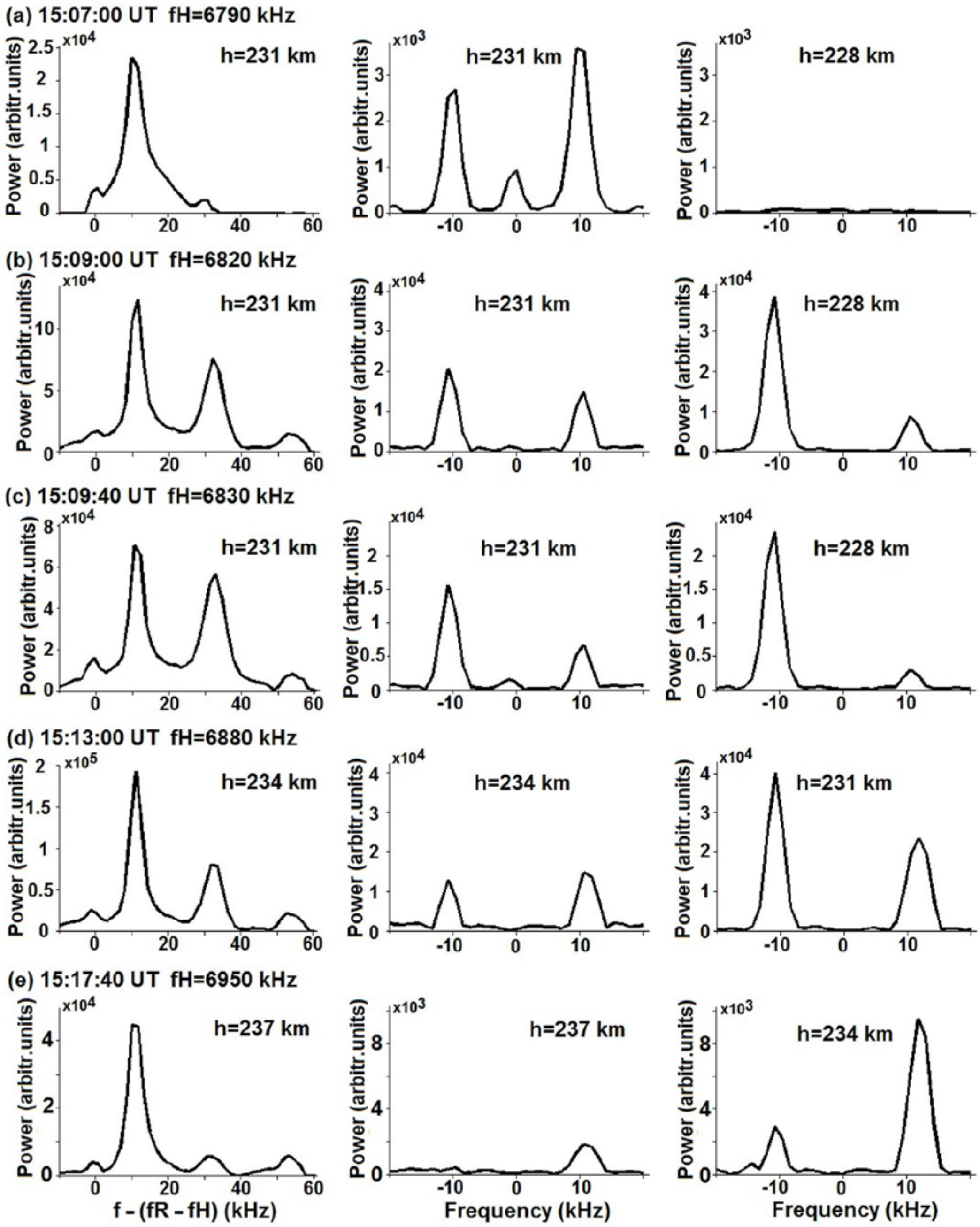
(a) 15:07:00 UT fH=6790 kHz
h=231 km
h=231 km
h=228 km
(b) 15:09:00 UT fH=6820 kHz
h=231 km
h=231 km
h=228 km
(c) 15:09:40 UT fH=6830 kHz
h=231 km
h=231 km
h=228 km
(d) 15:13:00 UT fH=6880 kHz
h=234 km
h=234 km
h=231 km
(e) 15:17:40 UT fH=6950 kHz
h=237 km
h=237 km
h=234 km
Power (arbitr.units)
f – (fR – fH) (kHz)
Frequency (kHz)
Frequency (kHz)

Figure 5.

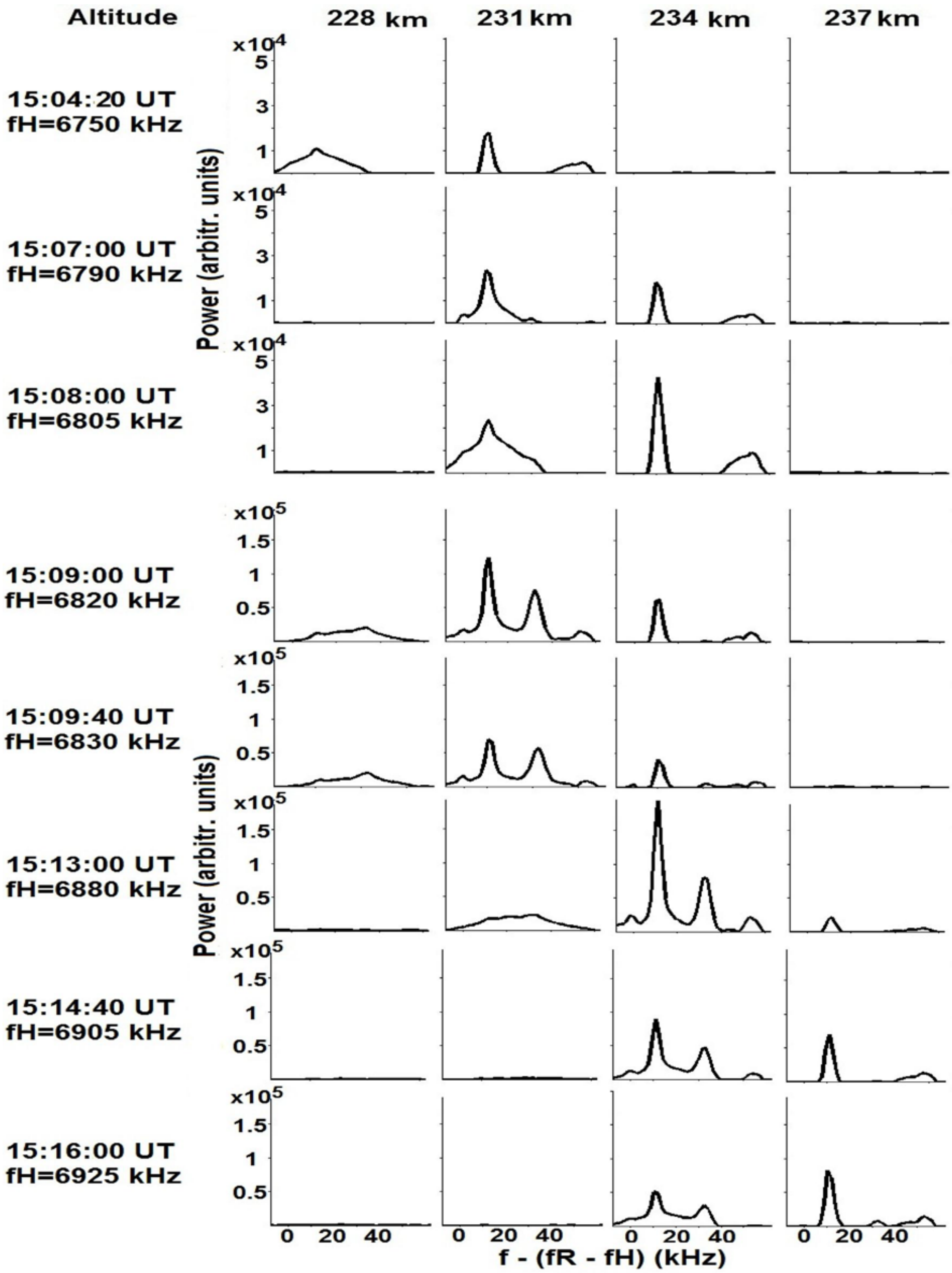

Altitude
228 km
231 km
234 km
237 km
15:04:20 UT
fH=6750 kHz
15:07:00 UT
fH=6790 kHz
15:08:00 UT
fH=6805 kHz
15:09:00 UT
fH=6820 kHz
15:09:40 UT
fH=6830 kHz
15:13:00 UT
fH=6880 kHz
15:14:40 UT
fH=6905 kHz
15:16:00 UT
fH=6925 kHz
Power (arbitr. units)
x10^4
x10^5
f - (fR - fH) (kHz)

Figure 6.

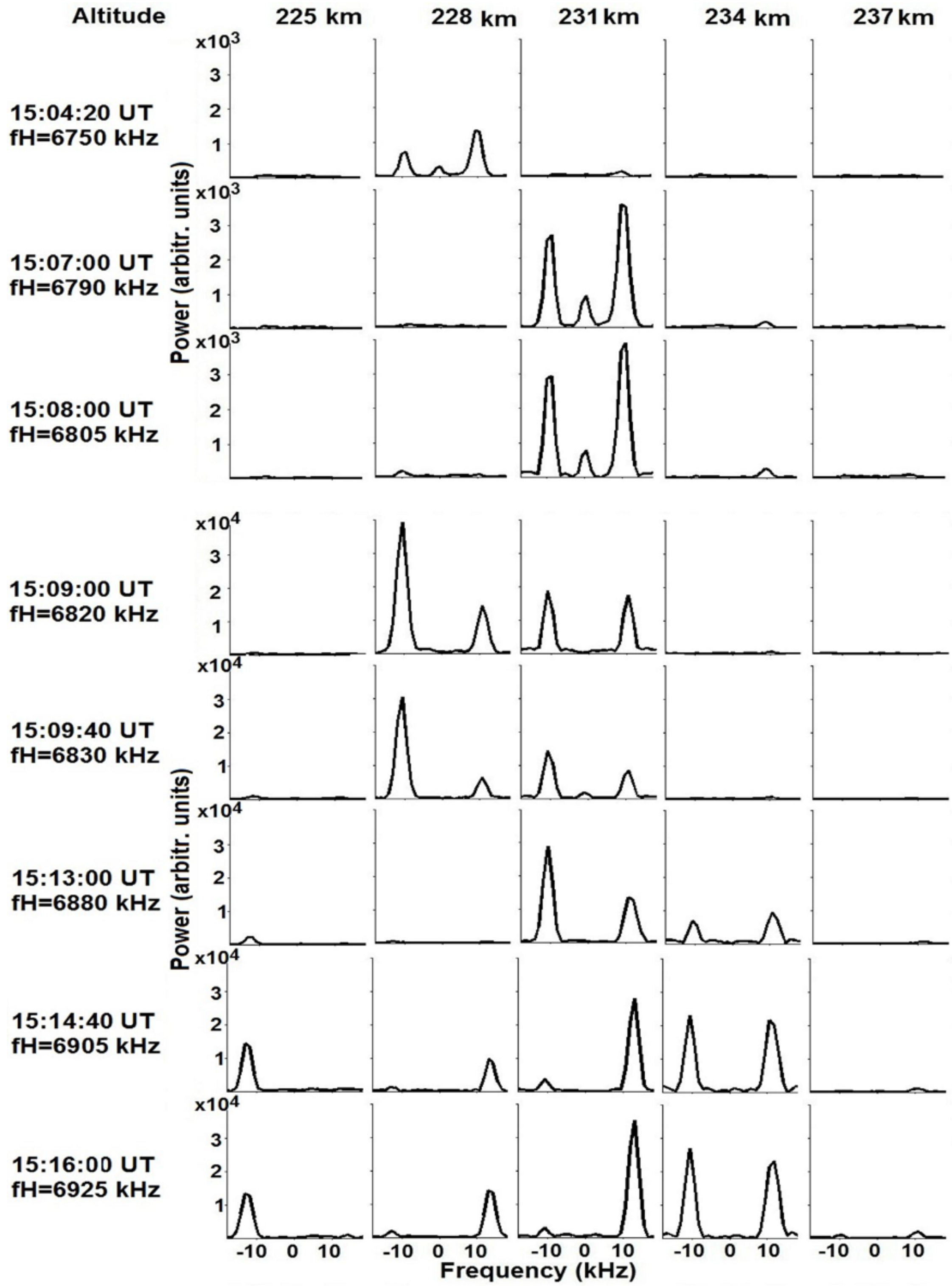
Altitude
225 km
228 km
231 km
234 km
237 km
15:04:20 UT
fH=6750 kHz
15:07:00 UT
fH=6790 kHz
15:08:00 UT
fH=6805 kHz
15:09:00 UT
fH=6820 kHz
15:09:40 UT
fH=6830 kHz
15:13:00 UT
fH=6880 kHz
15:14:40 UT
fH=6905 kHz
15:16:00 UT
fH=6925 kHz
Power (arbitr. units)
x10^3
x10^4
Frequency (kHz)

Figure 7.

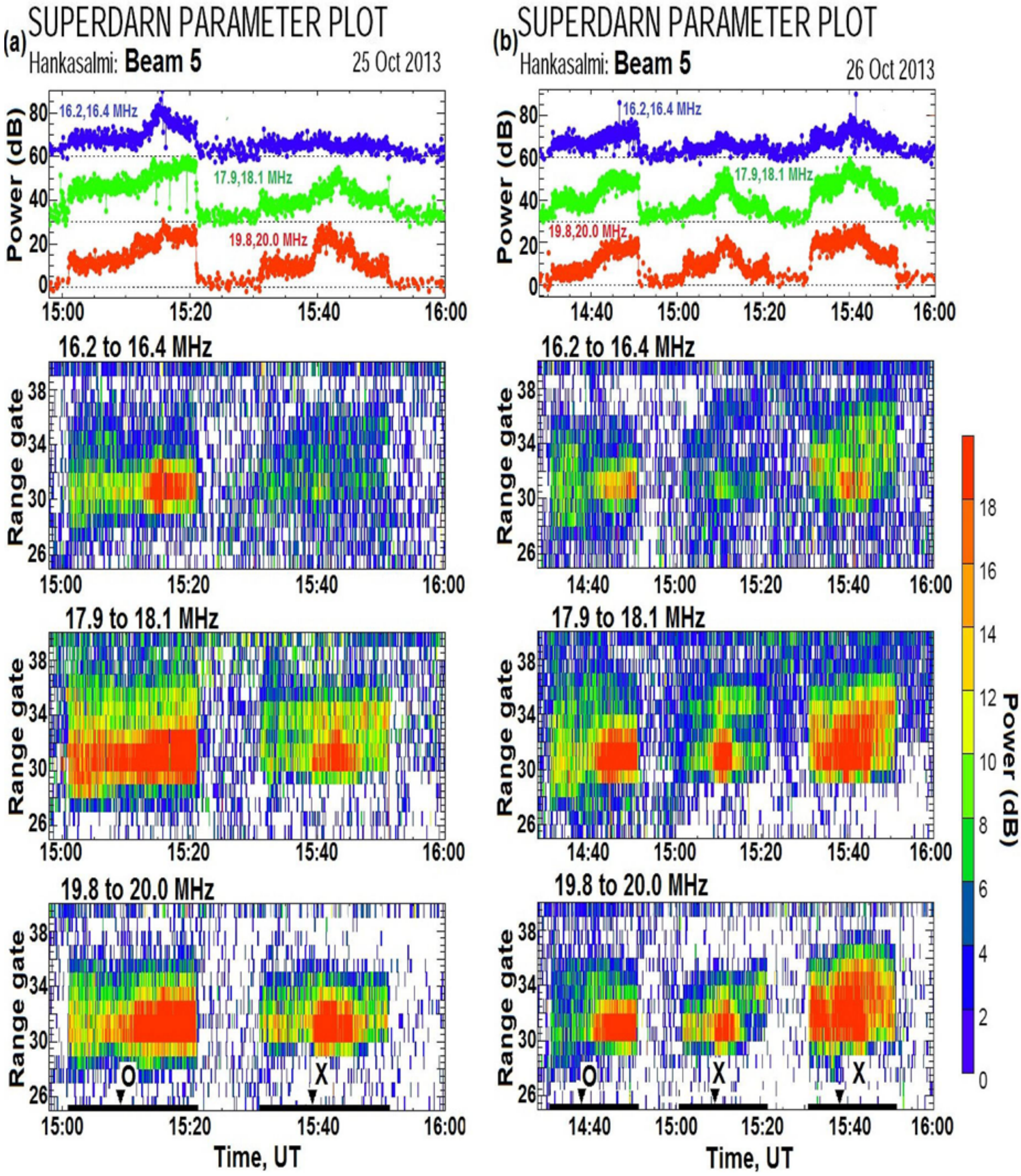

(a)
SUPERDARN PARAMETER PLOT
Hankasalmi: Beam 5
25 Oct 2013
16.2,16.4 MHz
17.9,18.1 MHz
19.8,20.0 MHz
Power (dB)
16.2 to 16.4 MHz
17.9 to 18.1 MHz
19.8 to 20.0 MHz
Range gate
O
X
Time, UT
(b)
SUPERDARN PARAMETER PLOT
Hankasalmi: Beam 5
26 Oct 2013
16.2,16.4 MHz
17.9,18.1 MHz
19.8,20.0 MHz
Power (dB)
16.2 to 16.4 MHz
17.9 to 18.1 MHz
19.8 to 20.0 MHz
Range gate
O
X
X
Time, UT
Power (dB)

Figure 8.